Exploring an Anti-Crystal Engineering Approach to the Preparation of Pharmaceutically Active Ionic Liquids

ARTICLE *in* CRYSTAL GROWTH & DESIGN · DECEMBER 2008

Impact Factor: 4.89 · DOI: 10.1021/cg8009496

5 AUTHORS, INCLUDING:

Pamela M Dean
Monash University (Australia)
22 PUBLICATIONS **282** CITATIONS
SEE PROFILE

Masahiro Yoshizawa-Fujita
Sophia University
93 PUBLICATIONS **3,284** CITATIONS
SEE PROFILE

Janet Scott
University of Bath
106 PUBLICATIONS **3,098** CITATIONS
SEE PROFILE

CRYSTAL GROWTH & DESIGN
2009
VOL. 9, NO. 2
1137–1145

Exploring an Anti-Crystal Engineering Approach to the Preparation of Pharmaceutically Active Ionic Liquids

Pamela M. Dean, Jelena Turanjanin, Masahiro Yoshizawa-Fujita,† Douglas R. MacFarlane, and Janet L. Scott*

School of Chemistry, Monash University, Wellington Road, Clayton, Victoria 3800, Australia

Received August 27, 2008; Revised Manuscript Received November 23, 2008

ABSTRACT: A series of salts, some of which are ionic liquids, are prepared from cations and anions drawn from Active Pharmaceutical Ingredients (APIs) and Generally Recognized As Safe (GRAS) materials. Using the solid-state structures of the crystalline salts as a basis, an anti-crystal engineering approach to the preparation of "Active Ionic Liquids" (AILs) is explored.

Introduction

The physical form of a drug substance is of great importance as it directly affects the manner in which the material is formulated and presented to the consumer, as well as influencing more fundamental characteristics such as solubility and dissolution rate, which, in turn, impact on bioavailability. These factors, as well as the considerable financial gains to be realized by effective patent protection of new physical forms, have resulted in a flurry of activity in screening for novel solid forms, including salts, polymorphs, pseudopolymorphs (or solvates), and co-crystals.[1] There are myriad examples in the scientific literature, with doubtless many more in the closed research files of large pharmaceutical companies. More than 50% of drug compounds are marketed are salts,[2] and the exploitation of differences in the number of crystal forms, interconversion of these, and the attendant changes in physical properties are not insignificant. In addition, the counterion is sometimes little more than ionic "ballast" as the identity of this often follows from synthesis or purification routes, rather than rational choice or screening.

Recently Rogers and co-workers have reported ionic liquids formed from active pharmaceutical ingredients (APIs) and have commented on the potential scope of this, to date poorly exploited, drug phase.[3] (The term "ionic liquid" is now widely accepted to describe salts with melting points <100 °C, although some authors distinguish a subset of these salts as Room Temperature Ionic Liquids or RTILS, that is, those salts that are in the liquid phase at ambient temperature.) Clearly a salt that does not exhibit a crystalline phase will not be bedevilled by polymorphism, but there are further advantages to be realized and exploited in the delivery of the API. In particular, a non-crystalline salt in a liquid or glassy phase will almost certainly exhibit the enhanced solubility exhibited by amorphous phases. This concept bears further discussion as it is potentially one of the most important advantages of the formulation of APIs as ionic liquid phases. A schematic comparison of the accessible phases and the relative free energy of each is presented in Figure 1.[4]

A significant number of drugs currently on the market are formulated as amorphous materials, and the most common means of preparing the amorphous phase is by quenching: rapid cooling from the melt; rapid precipitation from solution (for example on addition of an antisolvent); spray drying; flash evaporation; lyophilisation; or, indeed, any method that allows the disordered glassy phase to be "frozen in" before nucleation and growth lead to the appearance of crystals of the API.[5] Unfortunately, in cases where a stable crystalline form exists at ambient temperature, ΔG_f° for the crystalline phase is *lower* than that for the amorphous material formed by quenching, and thus quenching results in trapping in a form that is not the thermodynamically most stable phase at that temperature, Figure 1a. Thus, any event that initiates nucleation may lead to growth of a crystalline phase at the expense of the amorphous glass. Such nucleation initiators may include heating (yielding a plastic phase that then crystallizes) or localized shock, such as that applied during size reduction (grinding) or formulation. In some cases, even the desired increased solubility leads immediately to crystallization of a stable crystalline phase. Thus, upon addition of amorphous Indomethecin to water, dissolution of the amorphous material yields a localized concentration of the drug that is higher than its saturation limit, leading to immediate crystallization.[4]

Here, we consider the concept of ionic liquids formed from API ions in the light of the extensive literature on crystalline drug forms, "crystal engineering"[6,7] and the exploitation of "supramolecular synthons";[8] concepts which have been applied in developing strategies for increasing solubility of drug compounds[9] and in the choice of co-crystal formers[10] for poorly soluble drugs,[11] such as carbamazepine.[12] Emphasis must be placed on the preparation of a salt that has an amorphous phase as its thermodynamically most stable form (in the temperature range of interest), that is, a salt that is a liquid or glass, but NOT a supercooled liquid, such as that depicted in Figure 1b. A less preferred, but nonetheless effective form, would be one with T_{fusion} for the stable form below the T of interest, as in Figure 1c.

Combining an understanding of the effect of robust supramolecular synthons on the process of crystallization, with the concepts familiar to chemists working with ionic liquids, we propose the development of an "anti-crystal engineering" approach to the synthesis of Active Ionic Liquids (AILs). This would comprise identifying and intentionally *avoiding* the pairing of cations and anions that might yield common supramolecular synthons, with the goal of decreasing the likelihood of crystallization of salt. This "anti-crystal engineering" approach is postulated as a means of narrowing the search for AILs to cation and anion pairs that have a higher likelihood of NOT crystallizing. Thus, herein, we begin to illustrate this approach by preparing and analyzing a series of API salts some of which crystallize readily, while others are AILs and remain in an

* To whom correspondence should be addressed. E-mail: janet.scott@sci.monash.edu.au
† Current address: Department of Chemistry, Sophia University, 7-1 Kioi-cho, Chiyoda-ku, Tokyo 102-8554, Japan.

10.1021/cg8009496 CCC: $40.75
Published on Web 12/23/2008

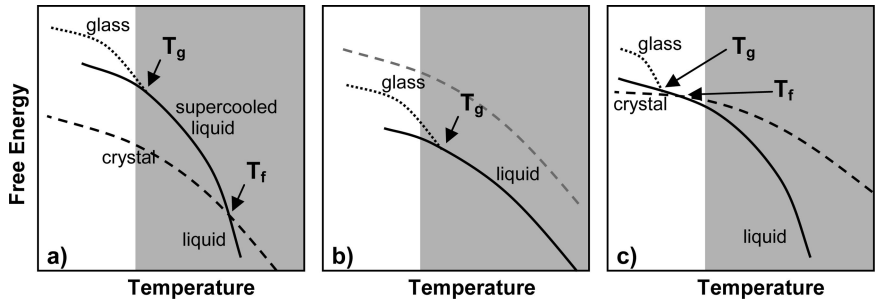

Figure 1. Simplified schematic of free energy vs temperature for (a) a compound with a stable crystalline phase, which may be supercooled to form an unstable supercooled liquid or glass and thus exhibits a tendency to crystallize when the system is perturbed; (b) a compound without a stable crystalline phase [or (gray dashed line) with a crystalline phase that is at a higher energy than the liquid phase over the entire region shown], such as an ionic liquid; (c) a compound with T_{fusion} below ambient temperature, which has a stable crystalline phase, but only at sub-ambient temperatures.

Chart 1. Pharmaceutically Active Cations[a]

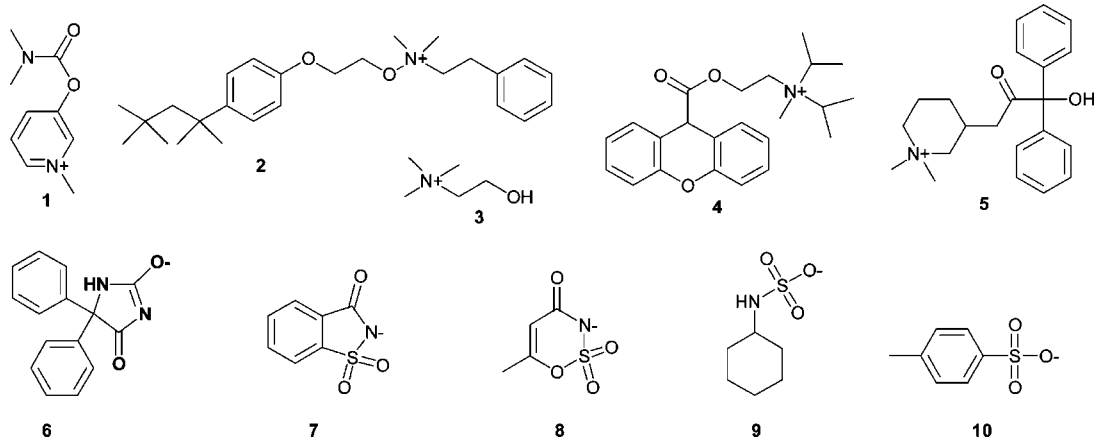

[a] 3-(Dimethylaminocarbonyloxy)-1-methylpyridinium cation (pyridostigmine) **1**; benzyl-dimethyl[2-[2-[4-(1,1,3,3-tetramethylbutyl)phenoxy]ethoxy]ethyl] ammonium cation (benzethonium) **2**; methyl-bis(1-methylethyl)-[-(9H-xanthen-9-carbonyloxy)ethyl ammonium cation (propantheline) **4**; (1,1-dimethyl-3,4,5,6-tetrahydro-2H-pyridin-3-yl) 2-hydroxy-2,2-diphenyl-acetate cation (mepenzolate) **5**; and anion: 5-oxo-4,4-diphenyl-1H-imidazol-2-olate cation (phenytoin) **6** are combined with sweetener anions: saccharinate **7**, acesulfamate **8**, and cyclamate **9** or with the GRAS ions: choline **3**, or *p*-toluenesulfonate **10**.

amorphous glass or liquid form in spite of vigorous attempts to bring about crystallization.

Results and Discussion

A small group of cations and anions selected from API salts and the Generally Recognized As Safe (GRAS) list were chosen for combination to yield salts containing active ions (Chart 1). Pyridostigmine **1** is an acetylcholinesterase inhibitor and is marketed as the slightly soluble crystalline Br^- salt, branded as Mestinon; benzethonium **2** is used in the form of the Cl^- salt as an anti-infective agent in many topical antiseptic gels and is marketed under many trade names, such as Salanine; propantheline **4**, a muscarinic acetylcholine receptor antagonist, is marketed in its Br^- salt form as Pro-Banthine; mepenzolate **5** is used as a skeletal muscle relaxant and is currently administered in the crystalline Br^- salt form generally known as Cantil; and phenytoin **6**, as its sodium salt, is an antiepileptic marketed variously as Phenytek, Dilantin, Eptoin, or Epanutin. The choline cation **3**, *p*-toluenesulfonate anion **10**, and sweetener anions saccharinate **7**, acesulfamate **8**, and cyclamate **9** are all to be found in the GRAS list and are potential counterions that are known to form ionic liquids in other cases. All cations contain tetra-alkylated ammonium or alkylpyridinium moieties commonly found in ionic liquids, and all anions, bar phenytoin, have been previously used in the preparation of ionic liquids.[13−18]

The salts were prepared via ion metathesis reactions commonly used in ionic liquid synthesis and were analyzed, with respect to purity, with particular attention to residual ions such as Br^-. Combinations of these ions yielded a number of isolable salts (Table 1), including three that exhibit no detectable phase changes ascribable to the existence of crystalline phases, on Differential Scanning Calorimetric (DSC) analysis. Melting, crystallization, and glass transition events were inferred from endotherms, exotherms, or changes in heat capacity detected by DSC analysis in multiple quenching, heating, and cooling experiments. In all cases at least three repeated heating and cooling cycles in the range −100 to 200 °C were effected. Positive identification of AILs (as with all ionic liquids) is not as simple as isolation of a salt that is oily or glassy at room temperature, as such materials may simply be solids in which crystallization is frustrated by the presence of impurities, or quenched amorphous phases, that is, supercooled melts. Thus, in addition to the low temperature DSC experiments described above, various attempts were made to induce crystallization: bulk (2 g) samples of the pure liquids were stored and examined over extended periods (4 months or more) for signs of crystallization, and standard crystal growth techniques, such as dissolution in suitable solvents (including wet solvents) followed by slow cooling or slow evaporation, were employed to test the integrity of the liquid state.

Table 1. Glass Transition Temperatures or Melting Points of Salts Prepared and As Reported for the Marketed Salts and Starting Materials

salt		T_{glass} / °C	T_{fusion} / °C
pyridostigmine bromide[a]	**1**·Br	*b*	154−157[c]
benzethonium chloride[a]	**2**·Cl	*b*	164−166[c]
choline chloride[a]	**3**·Cl	*b*	302−305 (dec.)[c]
propantheline bromide[a]	**4**·Br	*b*	159−161[c]; 165−169[d]
mepenzolate bromide[a]	**5**·Br	*b*	228−229[c]; 232−235[d]
phenytoin sodium[a]	Na·**6**	*b*	>350 (dec.)[c]
sodium saccharinate[a]	Na·**7**	*b*	>250 (dec.)[c]
potassium acesulfamate[a]	K·**8**	*b*	225−229[c]
sodium cyclamate[a]	Na·**9**	*b*	262−265[c]
silver *p*-toluenesulfonate[a]	Ag·**10**	*b*	192−194[c]
pyridostigmine saccharinate	**1**·**7**	4[e]	94−96[d]
benzethonium saccharinate	**2**·**7**	−4	
choline phenytoin	**3**·**6**	*f*	215−217[d]
propantheline saccharinate	**4**·**7**	18[e]	133−135[d]
propantheline acesulfamate	**4**·**8**	−20	
propantheline cyclamate	**4**·**9**	20[e]	133−137[d]
propantheline *p*-toluenesulfonate	**4**·**10**	7	
mepenzolate saccharinate	**5**·**7**	53[e]	187−189[d]
mepenzolate acesulfamate	**5**·**8**	34[e]	135−137[d]

[a] Starting material. [b] Not measured. [c] Literature. [d] DSC measurement. [e] Tg values measured on DSC heating cycles subsequent to melt, indicative of supercooling; in all cases samples were analyzed over 3 heating/cooling cycles in the range −100 to 200 °C (or 220 and 240°C for **3**·**6** and **5**·Br, respectively). [f] No T_g detected on DSC cool/heat cycles, compound recrystallizes on cooling.

It is important to distinguish between quenched amorphous phases, obtained by rapidly freezing a salt (for example by rapid cooling or solvent quenching of a melt) and salts that do not exhibit a crystalline phase, such as propantheline *p*-toluenesulfonate (**4**·**10**), which DSC trace is presented in Figure 2a. The former is trapped in a metastable state with a higher free energy than that of the crystalline form, so that events promoting nucleation, such as shock or abrasion common during formulation, may cause such salts to crystallize. By contrast, a salt without a crystalline phase (or with a sub-ambient melting point) is in the thermodynamically most stable phase as a liquid or glass at ambient temperature. Thus, **2**·**7**, **4**·**8**, and **4**·**10** are AILs while **1**·**7**, **4**·**7**, **4**·**9**, **5**·**7**, and **5**·**8** are merely crystalline salts with a tendency to supercool (which may lend themselves to formulation as amorphous materials as per many other pharmaceutical salts) but are *not* AILs.

The tendency of many of these salts to form supercooled amorphous glassy phases is reflected in the presence of glass transitions and lack of clear endothermic melting events on the second DSC heating cycle, as illustrated for propantheline saccharinate (**4**·**7**) in Figure 2b. This is reflected in the very slow crystallization of some of these salts: **1**·**7**, **4**·**9**, and **5**·**8** slowly crystallized from bulk samples over a time scale of weeks to months. Indeed, such supercooling led us initially to erroneously assign propantheline saccharinate (**4**·**7**) as an ionic liquid as, in early experiments, no crystalline product was obtained and no melting point detected in multiple DSC quench/heat/cool/heat experiments; however, crystals slowly formed in a stored bulk sample after many months. We will return to this discussion when we consider the crystal structures of the salts. The salts prepared all exhibit lower melting points than the chloride or bromide salts (of the cations) or sodium, potassium, or silver salts (of the anions) used as starting materials, Table 1, which lends some credence to the choice of counterions as bulky, unsymmetrical, and/or charge diffuse ions.

To begin exploration of the anti-crystal engineering approach to choosing cation/anion combinations, which would entail identifying robust supramolecular synthons, such as strong hydrogen bonds (usually considered to impart a tendency toward crystallization[19,20]) that should be avoided in the quest for AILs, we chose to prepare a range of salts, including some expected to crystallize. If one were to adopt a highly reductionist approach, one might formulate the following hypothesis: complementary hydrogen bond donor and acceptor groups are likely to lead to hydrogen bonded supramolecular synthons, which promote order and thus crystallization, that is, will not form AILs. This hypothesis may then be tested. Functional groups with the potential for formation of such synthons may be counted, and a crude prediction made of which pairs are more or less likely to crystallize because of the influence of strong hydrogen bonds, as is illustrated in Table 2.

Examining Table 2, it appears that our hypothesis, that is, "the existence of functional groups leading to hydrogen bonded synthons is likely to yield crystalline materials", holds (albeit as part of a very small sample), and all cation/anion combinations bearing both hydrogen bond donor and acceptor groups yield crystalline salts (**3**·**6**, **4**·**9**, **5**·**7**, and **5**·**8**). Such a result would have been predicted in the light of the extensive literature on the topic of hydrogen bonded supramolecular synthons. Gratifyingly, the pair which might be predicted to form the greatest number of strong, directional hydrogen bonds between different ions yields the salt with the highest melting point: choline phenytoin (**3**·**6**). Of greater interest, however, are those salts that are crystalline solids and yet do not (at first examination of individual ions) exhibit the capability to form hydrogen bonded synthons (**1**·**7** and **4**·**7**), and we turn to an examination

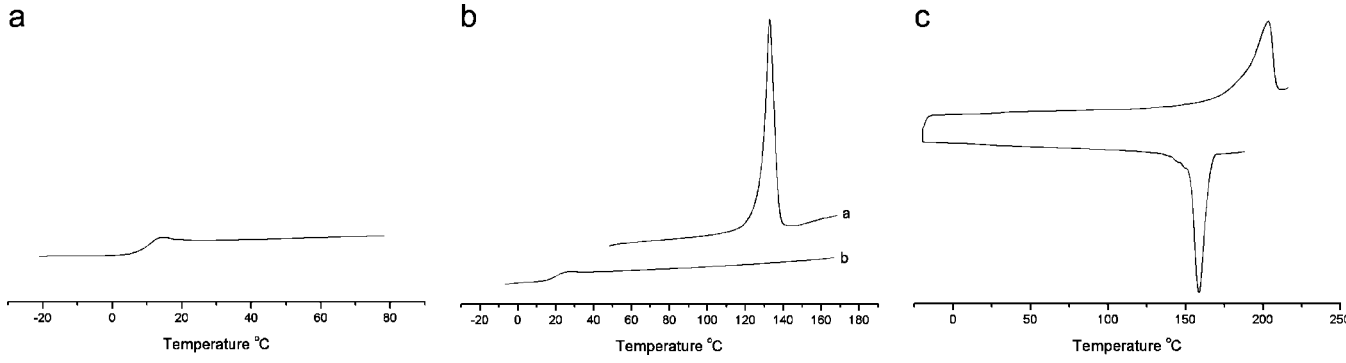

Figure 2. DSC traces of pure samples of (a) propantheline *p*-toluenesulfonate (**4**·**10**), an AIL, which exhibits a T_g only; (b) propantheline saccharinate (**4**·**7**), a crystalline salt that is prone to supercooling post melting (i.e., forms a typical amorphous salt phase), which is not an AIL; and (c) choline phenytoin (**3**·**6**), a highly crystalline salt, which does not supercool but instead recrystallizes during the cooling cycle. Note that while all samples were analyzed in multiple heating cooling cycles over the range −100 to 200 °C, selected data is presented here for the purposes of illustration. In addition, the DSC trace of **3**·**6** over the range −10 to −220 °C is presented.

Table 2. Hydrogen Bond Donor and Acceptor Groups Likely to Form Strong Hydrogen Bonds

	cation		anion		
salt	donors	acceptors	donors	acceptors	comments
1·7		R_3N C=O −O−		O=S=O −O− C=O N^-	low melting solid (mp 94−96 °C)
2·7		−O− −O−		O=S=O −O− C=O N^-	AIL
3·6	OH	OH	R_2NH	C=O =N− R_2NH $C-O^-$	−NH−C=O tend to form dimers; high mp solid (mp 215−217 °C); no tendency to supercool
4·7		−O− C=O −O−		O=S=O −O− C=O N^-	solid (mp 133−135 °C)
4·8		−O− C=O −O−		−O− O=S=O N^- C=O	AIL
4·9		−O− C=O −O−	R_2NH	R_2NH O=S=O $S-O^-$	solid (mp 133−137 °C)
4·10		−O− C=O −O−		O=S=O $S-O^-$	AIL
5·7	OH	OH C=O		O=S=O −O− C=O N^-	solid (mp 187−189 °C)
5·8	OH	OH C=O		−O− O=S=O N^- C=O	solid (mp 135−137 °C)

of representative crystal structures in an attempt to understand other more subtle interactions that may serve to promote crystallization and/or result in lattice energy stabilization. A number of crystal structures were obtained, and crystal and refinement data are summarized in Table 3. Specific details of crystal structure analysis and Oak Ridge Thermal Ellipsoid Plot (ORTEP) diagrams showing molecular numbering are contained in the Supporting Information.

Choline Phenytoin (3·6): Both Cation and Anion Bear Hydrogen-Bond Donor and Acceptor Functionality; High Probability of Crystallization. The amide moiety, NH−C=O, has been identified by Aakeröy and Zaworotko as likely to form a robust supramolecular synthon: the amide dimer,[21] and thus it is probably not surprising that this synthon manifests in these crystals as a dimer of the phenytoin ion, Figure 3a. A cation to anion hydrogen bond of the choline hydroxyl group to the phenytoin deprotonated nitrogen atom is also easily discerned by examination of intermolecular contacts, Figure 3b.

Examination of Hirshfeld fingerprint plots prepared using CrystalExplorer[22] reveal both strong and weak intermolecular interactions by providing a fingerprint plot of close contacts derived from Hirshfeld surface analysis, Figure 4. (The Hirshfeld surface is a 3D isosurface, which effectively defines the molecular volume in the crystal, as the surface is defined so that for each point on the surface "1/2 of the electron density is due to the spherically averaged noninteracting atoms comprising the molecule, and the other half is due to those comprising the

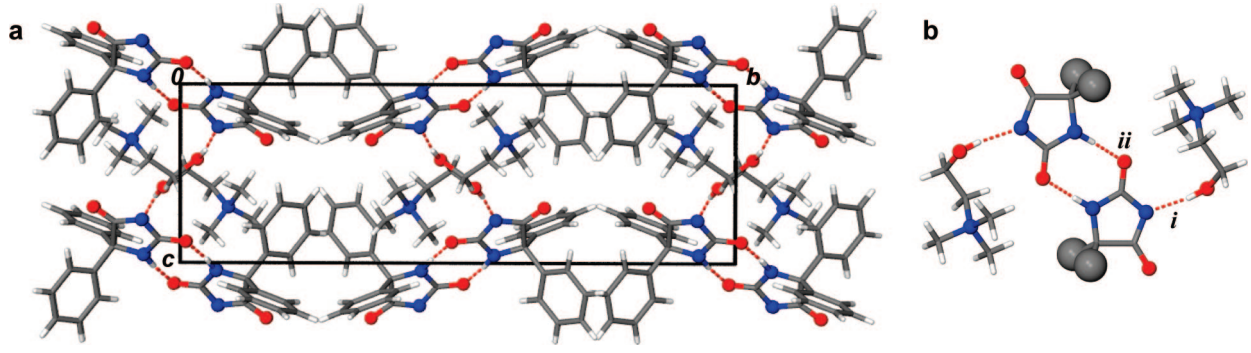

Figure 3. (a) Packing diagram of **3·6** viewed down 100. (b) Closeup of hydrogen bonded cation···anion/anion···cation dimers. Hydrogen bonds are indicated by dotted lines and N and O atoms depicted as spheres. Hydrogen bond geometry: (i) O1−H1···N1A *d* DH 0.89(3) Å; *d* D···A 2.804(2) Å; *d* H···A 1.92(3) Å; ∠ DHA 171.4(3)°; (ii) N2A-H2A···O1A(−*x*, −*y*, 2 − *z*) *d* DH 0.95(3) Å; *d* D···A 2.858(2) Å; *d* H···A 1.92(3) Å; ∠ DHA 173(2)°.

Table 3. Crystal and Refinement Data

	choline phenytoin **3·6**	propantheline cyclamate **4·9**	mepenzolate saccharinate **5·7**	propantheline saccharinate **4·7**
CCDC No.	658086	658085	658084	689108
empirical formula	$C_{20}H_{25}N_3O_3$	$C_{29}H_{42}N_2O_6S_1$	$C_{28}H_{30}N_2O_6S_1$	$C_{30}H_{34}N_2O_6S_1$
M_r	355.43	546.73	522.60	550.67
crystal system	monoclinic	triclinic	orthorhombic	monoclinic
space group	$P2_1/c$	$P\bar{1}$	$P2_12_12_1$	$P2_1/n$
a/Å	8.8575(2)	8.9636(3)	8.6732(1)	7.8305(16)
b/Å	25.5711(7)	12.5667(5)	11.5678(2)	13.694(3)
c/Å	8.6333(2)	12.7652(4)	24.6021(4)	25.404(5)
α/deg	90.0	88.606(2)	90.0	90.0
β/deg	111.604(1)	83.860(2)	90.0	96.20(3)
γ/deg	90.0	75.653 (2)	90.0	90.0
V/Å^3	1818.0(1)	1385.1(1)	2468.33(7)	2708.1(9)
Z'; Z	4	2	4	4
D_c/g.cm^{-3}	1.299	1.3107	1.4061	1.351
μ/mm^{-1}	0.090	0.163	0.179	0.167
refl. unique	4967	6809	7155	6037
refl. $I > 2\sigma(I)$	3084	6194	6716	1260
R_1/wR_2 [$I > 2\sigma(I)$]	0.0637/0.1566	0.0449/0.0901	0.0356/0.0900	0.1147/0.1537
R_1/wR_2 [all data]	0.1108/0.1876	0.0488/0.0939	0.0392/0.0929	0.4870/0.2587
GOF on F^2	0.980	1.020	1.115	0.911
parameters/restraints	335/0	511/0	340/0	357/0

rest of the crystal".[23]) The choline to phenytoin hydrogen bond results in a donor "spike" in the cation fingerprint plot (Figure 4a), which is complemented by a matching feature in the anion plot (Figure 4d) indicating the acceptor interaction. While the anion/anion hydrogen bonded pair results in symmetrical sharp features in Figure 4e, it is in detection of subtler interactions that 2D Hirshfeld fingerprint plots are particularly useful. Thus, CH···O short contacts between protons on carbon atoms α to the positively charged N atom result in smaller donor and acceptor "spikes", highlighted in panels b and e of Figure 4. CH···π interactions cation to anion produce "wings" visible in panels c and f of Figure 4, and the geometry of these interactions may be summarized: C3B−H3B(1 − x, −y, 2 − z)···centroid (C4A−C9A); d C−H 1.037 Å; d H···centroid 2.47 Å; ∠ CHcentroid 144.7 °; C3−H3A(−x, −y, 1 − z)···centroid (C10A−C15A); d C−H 0.947 Å; d H···centroid 2.58 Å; 164.8°.

Thus, in this highly crystalline salt, with no tendency to glass formation, all hydrogen bond interactions are maximized with the carbonyl O-atom of the anion acting as an acceptor for a number of weak (but concerted) C−H donors.

Propantheline cyclamate (4·9): Cation Contains Hydrogen-Bond Acceptor Functionality while Anion Bears Potential Hydrogen Bond Donors and Acceptors;

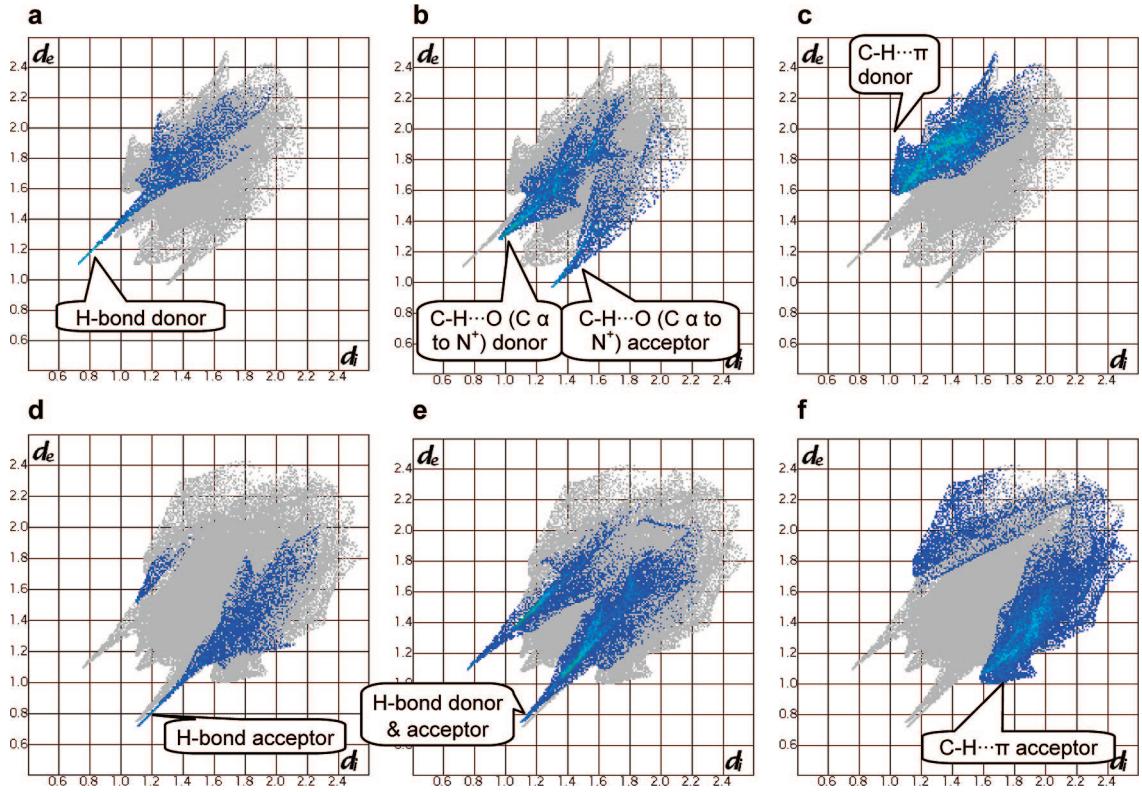

Figure 4. Decomposed Hirshfeld fingerprint plots[24] for **3·6**. Specific contacts are highlighted, while the entire 2D fingerprint is shown in gray. Top: Choline cation: (a) H···N contacts (and reciprocal i.e none); (b) H···O contacts (and reciprocal); (c) H···C contacts (and reciprocal, i.e., none). Bottom: Phenytoin anion. (d) N···H contacts (and reciprocal); (e) O···H contacts (and reciprocal); (f) H···C contacts (and reciprocal).

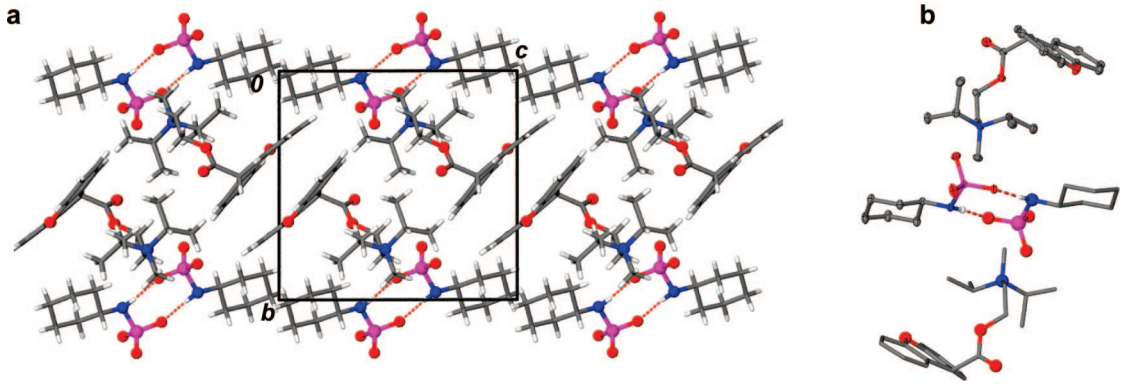

Figure 5. (a) Packing diagram of **4·9** viewed down [−100]. Anion/anion hydrogen bonds NH···O are indicated by dotted lines, and N, O, and S atoms depicted as spheres. (b) Closeup of hydrogen bonded anion dimer with attendant cations, asymmetric unit atoms are displayed as ellipsoids at the 50% probability level. H-bond geometry: N1A−H1A···O3A *d* DH 0.88(2) Å; *d* D···A 2.921(1) Å; *d* H···A 2.04(2) Å; ∠DHA 176(2)° (*d* O−S 1.460 Å).

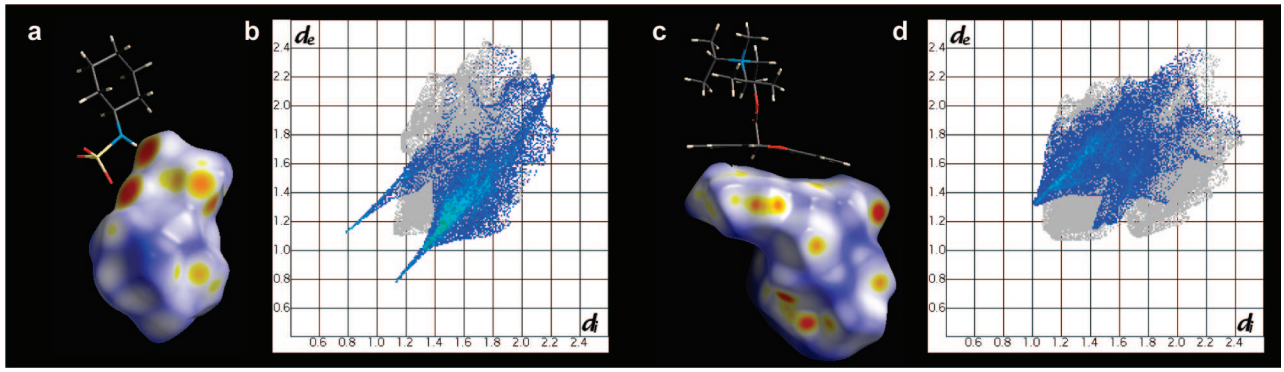

Figure 6. Propantheline cyclamate (**4·9**): (a) anion/anion dimers with one of the pair shown with its Hirshfeld surface (colors represent normalized d_e vs d_i plotted on the surface; "hot" colors reflect close contacts) and the other in stick mode with the accompanying 2D fingerprint plot in which the sharp symmetrical features associated with complementary hydrogen-bond donors are clearly visible; (b) decomposed 2D fingerprint plot with O−H···N contacts highlighted; (c) a cation/cation pair with one of the pair shown with its Hirshfeld surface (normalized d_e vs d_i plotted on the surface) and the other in stick mode, exhibiting complementary CH···π interactions with a small π···π component; (d) in the accompanying Hirshfeld fingerprint plot it is clear that the cation participates in no close contacts while the CH···π interactions are visible as characteristic "wings" in the donor region.

Predicted Cation/Anion and Anion/Anion Interactions. The propantheline cation (**4**) bears a number of hydrogen bond acceptors, while the cyclamate anion (**9**) contains one classical hydrogen-bond donor, leading one to expect anion/cation hydrogen bonds. While **4·9** crystallizes very slowly and has a distinct tendency to supercool, the melting point of 133−137 °C is only 30 °C (measured by DSC) below that of the marketed Br^- salt, and examination of the crystal structure reveals no anion/cation hydrogen bonding but instead the presence of anion/anion dimers, Figure 5. Examination of the Hirshfeld fingerprint plot for the anion in this structure reveals the supramolecular interactions in these dimers as typical symmetrical "horns" in the plot of d_e versus d_i, Figure 6. This suggests that the cyclamate anion is *not* a useful anti-crystal engineering building block since this tendency toward formation of anion dimers is likely to occur in many of its salts.

Mepenzolate saccharinate (5·7): Cation Bears Hydrogen-Bond Donor and Acceptor Functionality while Anion Bears Acceptors Only; Predicted Cation/Cation and Cation/Anion Interactions. Predictably, ion pairs in crystals of this salt exhibit cation to anion O−H···O═C hydrogen bonds as depicted in Figure 7.

Again, analysis of features observed in Hirshfeld surface fingerprint plots (Figure 8) provide information about both strong (and predictable) and weaker interactions. The cation/anion hydrogen-bond, O−H···O═C, is clearly indicated by the long horns in the donor region of Figure 8a, depicting cation H···O contacts, and the acceptor region of Figure 8c, depicting anion cation H···O contacts, while cation/cation C−H···π interactions result in the characteristic symmetrical "wings" noted in Figure 8b.

It is interesting to analyze more closely the dense set of points indicating O···H contacts in Figure 8c as these do not appear to be perfectly matched by H···O contacts in Figure 8a, instead there is a significant component because of N−C(α)−H···O interaction. The somewhat acidic protons of the carbon atoms α to N^+ are all disposed in close contact with oxygen atoms of the saccharinate anion as illustrated in Figure 8e. While CH···O hydrogen bonds are notoriously weak, there are *ten* such close contacts in each cation/anion pair, which would be expected to contribute significantly to attractive interactions between crystal components.

Thus, while the predicted cation/cation interactions are not exhibited in the crystal structure, cation/anion interactions are not limited to the hydroxyl to carbonyl hydrogen bond but include a large number of weaker C−H···O interactions.

Propantheline saccharinate (4·7): Both Cation and Anion Contain Hydrogen-Bond Acceptor Functionality Only; No Predicted Strong Cation/Anion Hydrogen

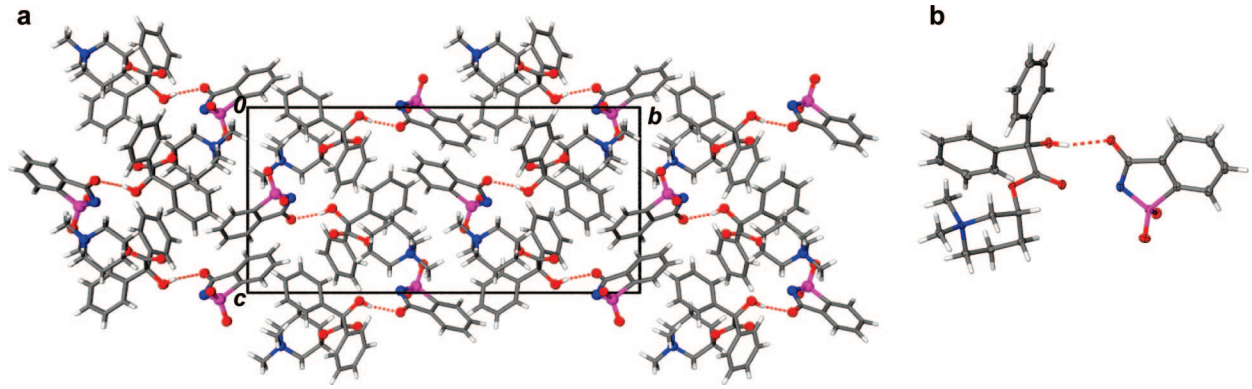

Figure 7. (a) Packing diagram of **5·7** viewed down [−100]. (b) Closeup view of hydrogen bonded cation/anion pair. N, O, and S atoms are depicted as spheres, and cation/anion hydrogen bonds OH···O are indicated by dotted lines. Hydrogen bond geometry: O1−H1···O3A: *d* D−H 0.85(3) Å; *d* D···A 2.752(2) Å; *d* H···A 1.94(3) Å; ∠ DHA 160(3)°.

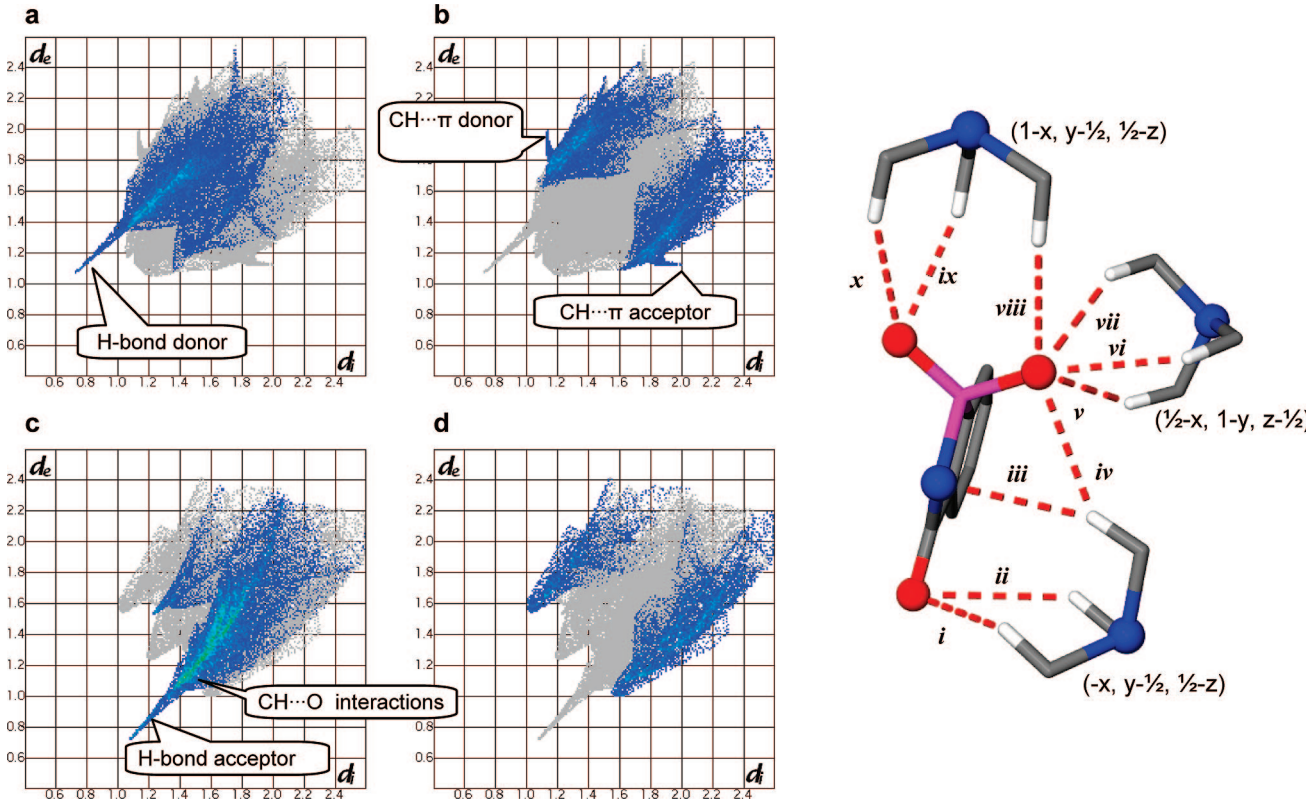

Figure 8. Hirshfeld fingerprint plots. Top: mepenzolate cation (**5**): (a) H···O contacts (including reciprocal contacts); (b) (**5**) H···C contacts (including reciprocal contacts). Bottom: saccharin anion (**7**): (c) H···O contacts (including reciprocal contacts); and (d) (**7**) H···C contacts (including reciprocal contacts). (e) Close contacts between protons borne on carbon atoms α to N^+ and anion O-atoms. Geometry of unique contacts: (i) H19A···O3A 2.52 Å; (ii) H20A···O3A 2.88 Å; (iii) N1A···H21C 2.71 Å; (iv) O1A···H21C 2.66 Å; (v) O1A···H18B 2.79 Å; (vi) O1A···H20C 2.53 Å; (vii) O1A···H21A 2.55 Å; (viii) O1A···H18A 2.61 Å; (ix) O2A···H20B 2.42 Å; (x) O2A···H19B 2.62 Å.

Bonds, Hence Possible AIL Former? Were hydrogen bonds the only driving force for crystallization in these salts, one would predict the combination of propantheline cation (**4**) and saccharinate anion (**7**), a cation/anion pair containing no classical hydrogen bond donor groups, to be a likely AIL former, but crystals of this salt *do* form in the supercooled melt (albeit extremely slowly). Single crystals examined were generally of poor quality, but the refined structure obtained is nonetheless suitable for analysis of packing and intermolecular distances. Analysis of the single crystal structure reveals no hydrogen bonds, as is illustrated in the packing diagram (Figure 9), and analysis of the 2D Hirshfeld fingerprint plots, Figure 10, reveals no short intermolecular contacts.

It is clear, from the packing diagram (Figure 9), that the "flat" face of the propantheline cation forms an offset $\pi\cdots\pi$ interaction with a symmetry related neighbor, and this is highlighted in panels e and f of Figures 10. Such $\pi\cdots\pi$ interactions are not readily discerned from examination of the features of the 2D Hirshfeld fingerprint plot as the atom···atom distances are typically of the order of 3.5 Å and thus obscured in the main body of points representing van der Waals interactions.

This salt may be described, somewhat anthropomorphically, as a "reluctant crystallizer", which nonetheless, once crystalline, exhibits a melting point well above ambient temperature. As with all salts, the most important contributor to lattice energy is, of course, Coulombic interactions between cation and anion,

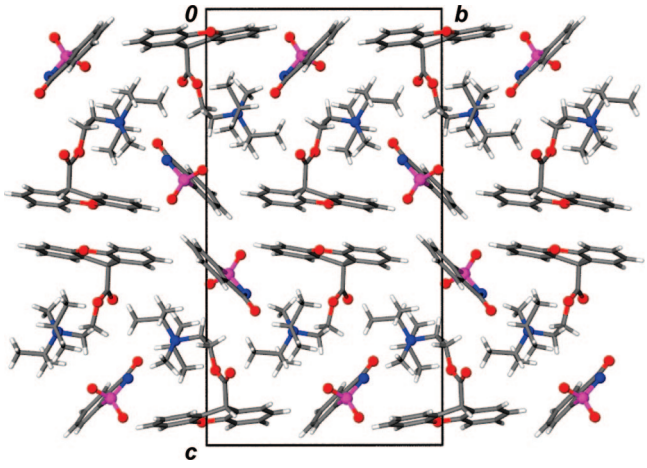

Figure 9. Packing diagram of **4·7** viewed down [1 0 0].

but the poor quality of the crystals formed, which contain a large number of crystal defects (reflected in high mosaicity values in crystal structure analysis) and the reluctance to crystallize, would seem to indicate that highly directional intermolecular (or interionic) interactions may be important in the process of crystallization.

Conclusion

AILs versus Crystalline Solids. Of this small library of salts prepared, all cation/anion combinations, with the potential to form classical hydrogen bonds (i.e., with ions bearing both hydrogen bond donor and acceptor groups), yielded salts that were crystalline solids (albeit with melting points lower than that of the marketed halide salts). In the single instance where both cation and anion bore both donor and acceptor groups, a high melting crystalline solid, with no tendency to supercool, resulted. Of the four cation/anion combinations with no opportunity for the formation of classical hydrogen bonds (because of a dearth of donor groups) one crystallized, while three formed AILs, which could not be induced to crystallize in spite of vigorous attempts. Propantheline saccharinate (**4·7**) appears to be the only salt, in this group, to counter our null hypothesis.

As postulated, complementary functional groups leading to supramolecular synthons associated with strong attractive intermolecular (or interionic) hydrogen bonded interactions must clearly be avoided in the preparation of AILs. However, as has been demonstrated, time and again, in crystal engineering, a wide range of other possible supramolecular synthons must be considered. Clearly, considerations of charge (in this study only monoanions and monocations were considered), charge separation, and shape are significant in determining whether or not a salt exists as a crystalline solid, and, indeed, lattice energy is the ultimate determinant of melting point (and crystallinity). Nonetheless we suggest that an "anti-crystal engineering" approach to the rational choice of ions for the preparation of non-crystallizing salts, including AILs, may provide another application for the knowledge gained in the study of crystal engineering by guiding the choice of complementary ions from the large number of candidates.

Experimental Section

Synthesis. Materials. Benzethonium chloride ($C_{27}H_{42}ClNO_2$, ≥99%, Sigma), choline chloride ($C_{15}H_{11}N_2O_2Cl_1$), mepenzolate bromide ($C_{21}H_{26}BrNO_3$, >99%, Sigma), propantheline bromide ($C_{23}H_{30}NO_3Br$, ≥97%, Sigma), pyridostigmine bromide ($C_9H_{13}BrN_2O_2$, >99%, Sigma), potassium acesulfame ($C_4H_4KNO_4S$, ≥99%, Fluka), silver p-toluenesulfonate ($AgCH_3C_6H_4SO_3$, ≥99%, Aldrich), sodium cyclamate ($C_6H_{12}NNaO_3S$, ≥99%, Merck), sodium 5,5-diphenylhydantoin ($NaC_5H_{14}NO$, >99%, Sigma), and sodium saccharinate

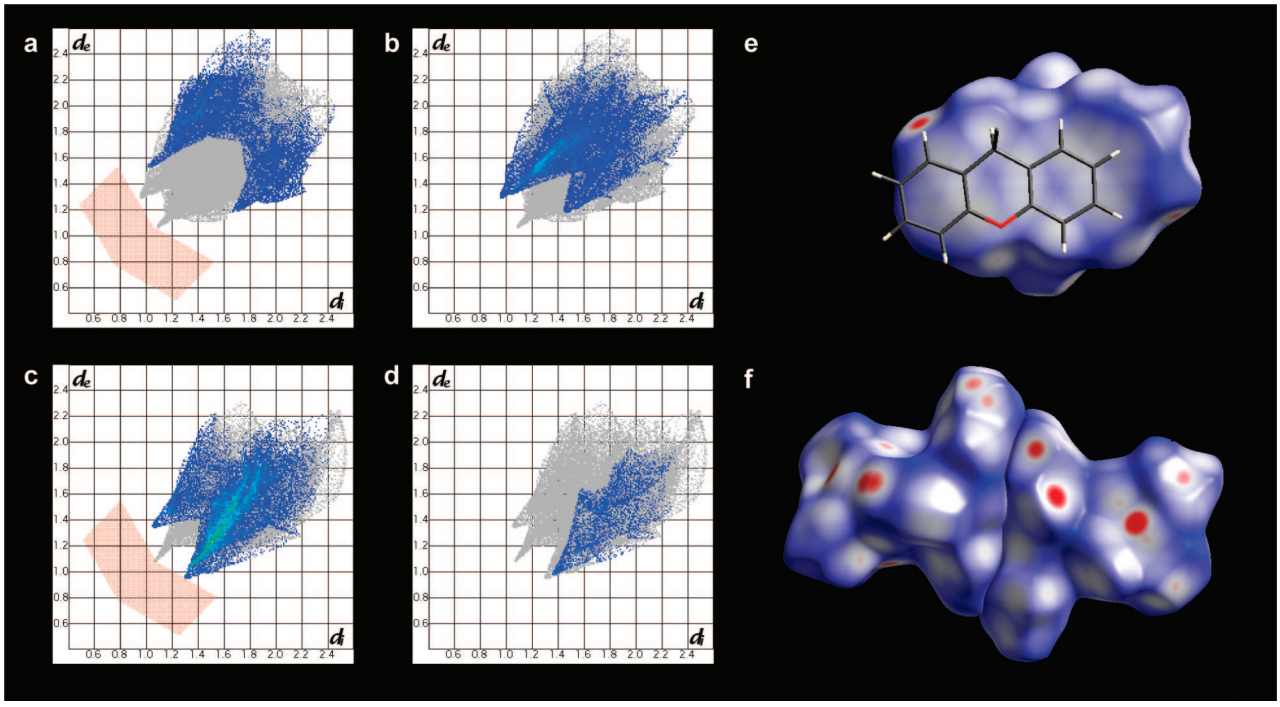

Figure 10. 2D Hirshfeld fingerprint plots for **4·7**. Top, propantheline cation (**4**): (a) C···H contacts (and reciprocal), (b) H···O contacts (and reciprocal). Bottom, saccharinate anion (**7**): (c) O···H contacts (and reciprocal); (d) N···H contacts (and reciprocal, i.e., none). No short-range contacts corresponding to hydrogen bonds, indicated by close approaches of atoms, are noted (these would fall in the pink shaded regions). (e) Hirshfeld surface for **4** with symmetry generated cation (aromatic moiety) overlaid; offset $\pi\cdots\pi$ interaction yields the multicenterd spoked pattern. (f) A pair of cations depicted as their Hirshfeld surfaces.

($C_7H_4NNaO_3S \cdot xH_2O$, ≥99%, Sigma) were used as received without further purification.

^{1}H NMR Spectroscopy. Proton nuclear magnetic resonance (^{1}H NMR) spectra were recorded at 200 or 300 MHz on a Bruker DPX-300 and Bruker DPX-200 spectrometers in the deuterated solvents indicated, which were supplied by Cambridge Isotope Laboratories.

MS-ESI. Electrospray Mass Spectrometry (ESI) was carried out on the Micromass Platform II API QMS Electrospray Mass Spectrometer with a cone voltage of 25 or 35 V, using methanol or acetonitrile as the mobile phases. Analyses were conducted in both positive (ES^+) and negative (ES^-) modes.

Halide Analysis. An Ionode S14 bromide selective electrode was used to measure the bromide content for **1·7**, **4·7**, **4·8**, **4·9**, **4·10**, **5·7**, and **5·8**. Calibration curves were constructed in the range 1 ppm to 1000 ppm for aqueous bromide solutions. The limit of detection corresponded to a Br^- ion concentration, in the sample, of 100 ppm and all salts prepared from Br^- salts exhibited residual bromide ion concentrations below this value, except **4·8** in which $Br^- = 210 \pm 10$ ppm. The absence of chloride ions in **2·7** and **3·6** was inferred from the absence of turbidity in a silver nitrate test.

General Synthetic Method. Details of the preparation of each salt and characterization data are provided in the Supporting Information. Salts were prepared by methathesis reactions of equimolar quantities of bromide or chloride salts of the cations with silver or sodium salts of the anions in suitable solvents. Silver salts of saccharinate, acesulfamate, and cyclamate were prepared prior to use and protected from light. Equimolar quantities of silver nitrate and sodium saccharinate, potassium acesulfamate or sodium cyclamate in distilled water were stirred overnight at room temperature. The resultant white precipitates were filtered, washed with cold distilled water, and dried in vacuo overnight at 50−55 °C to provide silver saccharinate, silver acesulfamate, or silver cyclamate.

Dry acetonitrile or dichloromethane were used as the reaction solvents allowing by-product salts to be removed by filtration post-reaction and, in the latter case, to facilitate washing to remove any trace impurities. In all cases, great care was taken to remove by-product salts and to test for halide impurities.

Differential Scanning Calorimetry. DSC experiments were performed on a T.A. Instruments Perkin-Elmer Q100. Samples of mass 5−20 mg were sealed in vented aluminum pans and placed in the furnace with a 50 mL/min dry nitrogen and analyzed in the range −100 to 200 °C (220 °C for **3·6**) at a scan rate of 10 °C min^{-1}. Heating/cooling cycles were repeated three times for each sample. The reference pan was an empty aluminum pan.

Crystallography. Crystallization of **3·6**, **4·9**, **5·7**, and **4·7** was observed in the metathesis product as detailed in the Experimental Section. The reflection intensity data were measured on a Bruker X8 APEX KAPPA CCD single crystal X-ray diffractometer (**4·9**, **5·7**) and a Nonius KAPPA CCD single crystal X-ray diffractometer (**3·6**, **4·7**), using graphite-monochromated Mo Kα radiation ($\lambda = 0.71073$ Å). Crystals were coated with Paratone N oil (Exxon Chemical Co., TX, U.S.A.) immediately after isolation and cooled in a stream of nitrogen vapor on the diffractometer. Structures were solved by direct methods using the program SHELXS-97 and refined by full matrix least-squares refinement on F^2 using SHELXL-97.[25] All non-hydrogen atoms were revealed in the E-map and subsequent difference electron density maps and thus placed and refined anisotropically. All hydrogen atoms were observed in difference syntheses and were either refined isotropically or placed in geometrically idealized positions and constrained to ride on their parent atoms with C−H distances in the range 0.95−1.00 Å and $U_{iso}(H) = xU_{eq}(C)$, where $x = 1.5$ for methyl and 1.2 for all other C atoms. Specific details of refinement are contained in the relevant CIF files.

Hirshfeld Analysis. The program CrystalExplorer (version 2.0 and 2.1)[22] was used to render all surfaces and fingerprint plots.

Acknowledgment. P.M.D. is grateful to Monash University for a Monash Graduate Scholarship and Monash International Postgraduate Research Scholarship, D.R.M. is grateful to the Australian Research Council for a Federation Fellowship. We also acknowledge the perspicacious referees' comments received, which enabled us to improve this manuscript in revision.

Supporting Information Available: Full details of synthesis and characterization for each salt; Ortep diagrams with molecular numbering and packing diagrams for **3·6**, **4·7**, **4·9**, and **5·7**, and X-ray crystallographic information files (CIF) for **3·6**, **4·7**, **4·9**, and **5·7**. This material is available free of charge via the Internet at http://pubs.acs.org.

References

(1) Peterson, M. L.; Hickey, M. B.; Zaworotko, M. J.; Almarsson, O. *J. Pharm. Pharm. Sci.* **2006**, *9*, 317–326.
(2) *Handbook of Pharmaceutical Salts: Properties, Selection, and Use*; Stahl, P. H., Wermuth, C. G., Eds.; Wiley VCH Verlag: Zürich, 2002.
(3) Hough, W. L.; Smiglak, M.; Rodriguez, H.; Swatloski, R. P.; Spear, S. K.; Daly, D. T.; Pernak, J.; Grisel, J. E.; Carliss, R. D.; Soutullo, M. D.; Davis, J. H., Jr.; Rogers, R. D. *New J. Chem.* **2007**, *31*, 1429–1436.
(4) These figures were inspired by that developed in Hancock, B. C.; Parks, M. *Pharm. Res.* **2000**, *17*, 397–404.
(5) (a) *Polymorphism in the pharmaceutical industry*; Hilfiker, R., Ed.;Wiley VCH:Weinheim, Germany, 2006. (b) *Polymorphism in Pharmaceutical Solids*, Brittain, H. G., Ed.; Marcel Dekker, Inc.: New York, 1999.
(6) Thalladi, V. R.; Satish Goud, B.; Hoy, V. J.; Allen, F. H.; Howard, J. A. K.; Desiraju, G. R. *Chem. Commun.* **1996**, 401–402.
(7) (a) Desiraju, G. R. *Angew. Chem., Int. Ed.* **2007**, *46*, 8342–8356. (b) Desiraju, G. R. *J. Mol. Sci.* **2003**, *656*, 5–15.
(8) Desiraju, G. R. *Angew. Chem., Int. Ed. Engl.* **1995**, *34*, 2311–2327.
(9) Blagden, N.; de Matas, M.; Gavan, P. T. *Adv. Drug Del. Rev.* **2007**, *59*, 617–630.
(10) Trask, A. V.; Jones, W. *Top. Curr. Chem.* **2005**, *254*, 41–70.
(11) Vishweshwar, P.; McMahon, J. A.; Bis, J. A.; Zaworotko, M. J. *J. Pharm. Sci.* **2006**, *95*, 499–516.
(12) Almarsson, O.; Zaworotko, M. *Chem. Commun.* **2004**, 1889–1896.
(13) Pernak, J.; Stefaniak, F.; Weglewski, J. *Eur. J. Org. Chem.* **2005**, 650–652.
(14) Carter, E. B.; Culver, S. L.; Fox, P. A.; Goode, R. D.; Ntai, I.; Tickell, M. D.; Traylor, R. K.; Hoffman, N. W.; Davis, J. H. *Chem. Commun.* **2004**, *63*, 0–631. Pernak, J.; Stefaniak, F.; Weglewski, J. *Eur. J. Org. Chem.* **2005**, 650–652.
(15) Pernak, J.; Syguda, A.; Mirska, I.; Pernak, A.; Nawrot, J.; Pradzynska, A.; Griffin, S. T.; Rogers, R. D. *Chem.—Eur. J.* **2007**, *13*, 6817–6827.
(16) Nockemann, P.; Thijs, B.; Driesen, K.; Janssen, C. R.; Van Hecke, K.; Van Meervelt, L.; Kossmann, S.; Kirchner, B.; Binnemans, K. *J. Phys. Chem. B* **2007**, *111*, 5254–5263.
(17) Golding, J.; Forsyth, S.; MacFarlane, D. R.; Forsyth, M.; Deacon, G. B. *Green Chem.* **2002**, *4*, 223–229.
(18) Fukaya, Y.; Iizuka, Y.; Sekikawa, K.; Ohno, H. *Green Chem.* **2007**, *9*, 1155–1157.
(19) While the term "crystal engineering" was probably first used by Schmidt in 1971, Schmidt, G. M. J. *Pure Appl. Chem.* **1971**, *27*, 647–678, the concept has been significantly broadened since.
(20) A number of excellent books on the topic exist, including: *Crystal Engineering: The Design and Application of Functional Solids*; Seddon, K. R, Zaworotko, M., Eds.; Kluwer Academic: Norwell, MA, 1999; *Frontiers in Crystal Engineering*; Tiekink, R. T., Vittal, J. Eds.; John Wiley and Sons Ltd.: Chichester, U.K., 2006.
(21) (a) Aakeröy, C. B.; Beatty, A. M.; Helfrich, B. A. *J. Chem. Soc., Dalton Trans.* **1998**, 1943–1946. (b) Aakeröy, C. B.; Beatty, A. M. *Chem. Commun.* **1998**, 1067–1068. (c) McMahon, J. A.; Bis, J. A.; Vishweshwar, P.; Shattock, T. R.; McLaughlin, O. L.; Zaworotko, M. J. *Z. Kristallogr.* **2005**, *220*, 340–350.
(22) McKinnon, J. J.; Spackman, M. A.; Mitchell, A. S. *Acta Crystallogr. Sect, B* **2004**, *60*, 627–668.
(23) Spackman, M. A.; McKinnon, J. J. *CrystEngComm* **2002**, *4*, 378–392.
(24) McKinnon, J. J.; Jayatilaka, D.; Spackman, M. A. *Chem. Commun.* **2007**, 3814–3816.
(25) Sheldrick, G. M. *Acta Crystallogr., Sect. A: Found. Crystallogr.* **2008**, *A64*, 112–122.

CG8009496